

The Cloud Radiative Response to Surface Warming Weakens Hydrological Sensitivity

Zachary McGraw^{1,2*}, Lorenzo M. Polvani^{1,3,4},
Blaž Gasparini⁵, Emily K. Van de Koot⁶, Aiko Voigt⁵

1 Department of Applied Physics and Applied Mathematics, Columbia University, New York, NY, USA

2 NASA Goddard Institute for Space Studies, New York, NY, USA

3 Department of Earth and Environmental Sciences, Columbia University, New York, NY, USA

4 Lamont-Doherty Earth Observatory, Columbia University, Palisades, NY, USA

5 Department of Meteorology and Geophysics, University of Vienna, Vienna, AT

6 Atmospheric, Oceanic and Planetary Physics, University of Oxford, Oxford, UK

* Corresponding author

Contents of this file:

Text S1

Figures S1 to S5

Supplementary References

Text S1. Examining the change in cloud radiative effects due to clear-sky responses

One probable influence of cloud radiative effects on HS results from the climatological presence of clouds affecting clear-sky radiative responses to warming, as is shown with ICON cloud locking output in panel iii of Fig. 4c. However, this is not an impact of cloud properties changing with warming, and hence is separate from the controls on HS focused on in the main text. The presently described interaction term is usually referred to as *cloud masking* (Soden et al., 2008; Yoshimori et al., 2020), although in Fig. 4c we depict the effect as local vertically-resolved radiative heating/cooling rather than, as is typical, impacts on TOA radiative flux. In ICON this interaction is consistent with high clouds warming and hence emitting more radiation to space when not accounting for their isothermal rise. In this case, cloud presence promotes increased emissivity at high altitudes where water vapor is thin, driving upper tropospheric radiative cooling. Conversely, this effect has the opposite impact at low altitudes, where cloud presence masks the enhanced emissivity from increased water vapor via Clausius-Clapeyron. In the global average the upper and lower tropospheric impacts nearly cancel, though this effect overall reduces the total impact of clouds on HS in the tropics (see triangle above ΔCRE in Figs. 4b and S4).

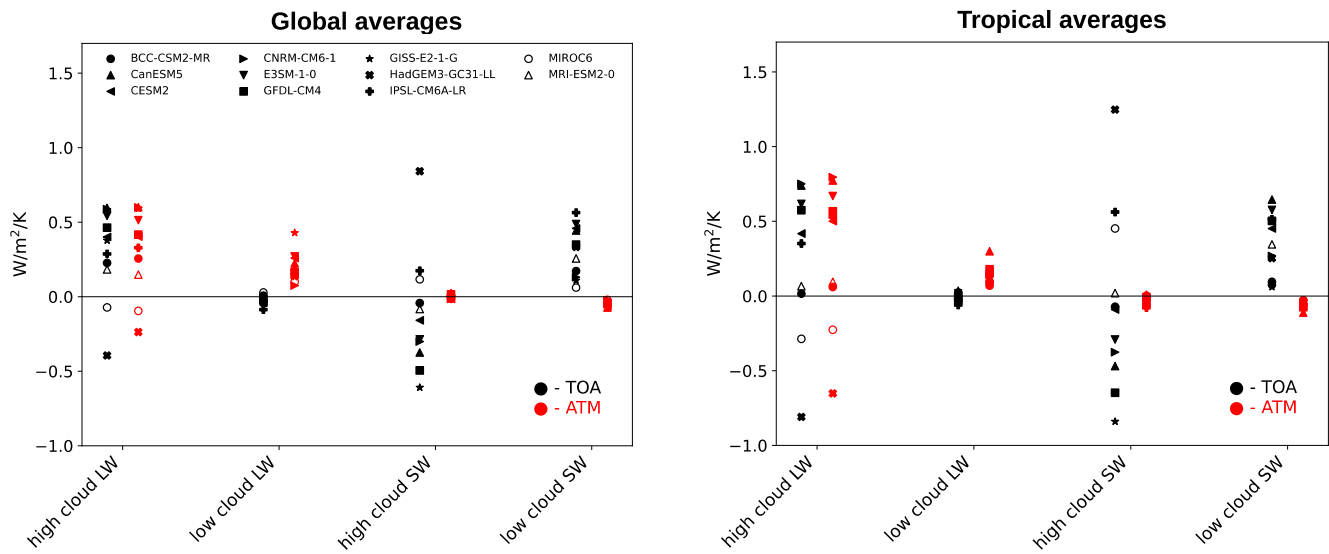


Figure S1. Kernel-derived feedbacks separated into shortwave and longwave components and shown for both top-of-atmosphere (TOA) and atmospheric (ATM) fluxes.

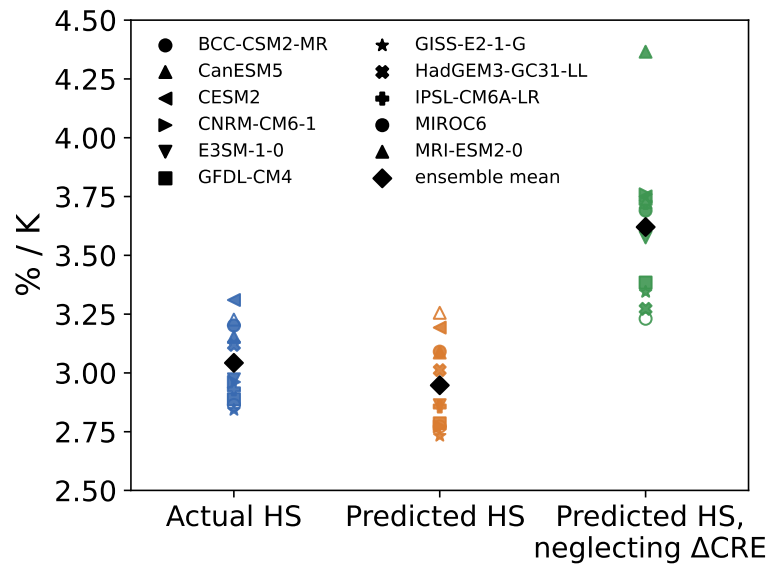


Figure S2. Global mean hydrological sensitivities across AMIP6 (as in Fig. 4a) compared to estimates based on the balancing terms in Eqn. 1. The “Predicted HS” is the percent per K change in the sum of CRE + R_{clear} + SH, compared to the control simulation (T1). In the right column, we also show the same without accounting for the Δ CRE, as $(\Delta R_{clear} + \Delta SH)/(R_{clear,T1} + CRE_{T1} + SH_{T1}) / \Delta T_{sfc} \times 100\%$.

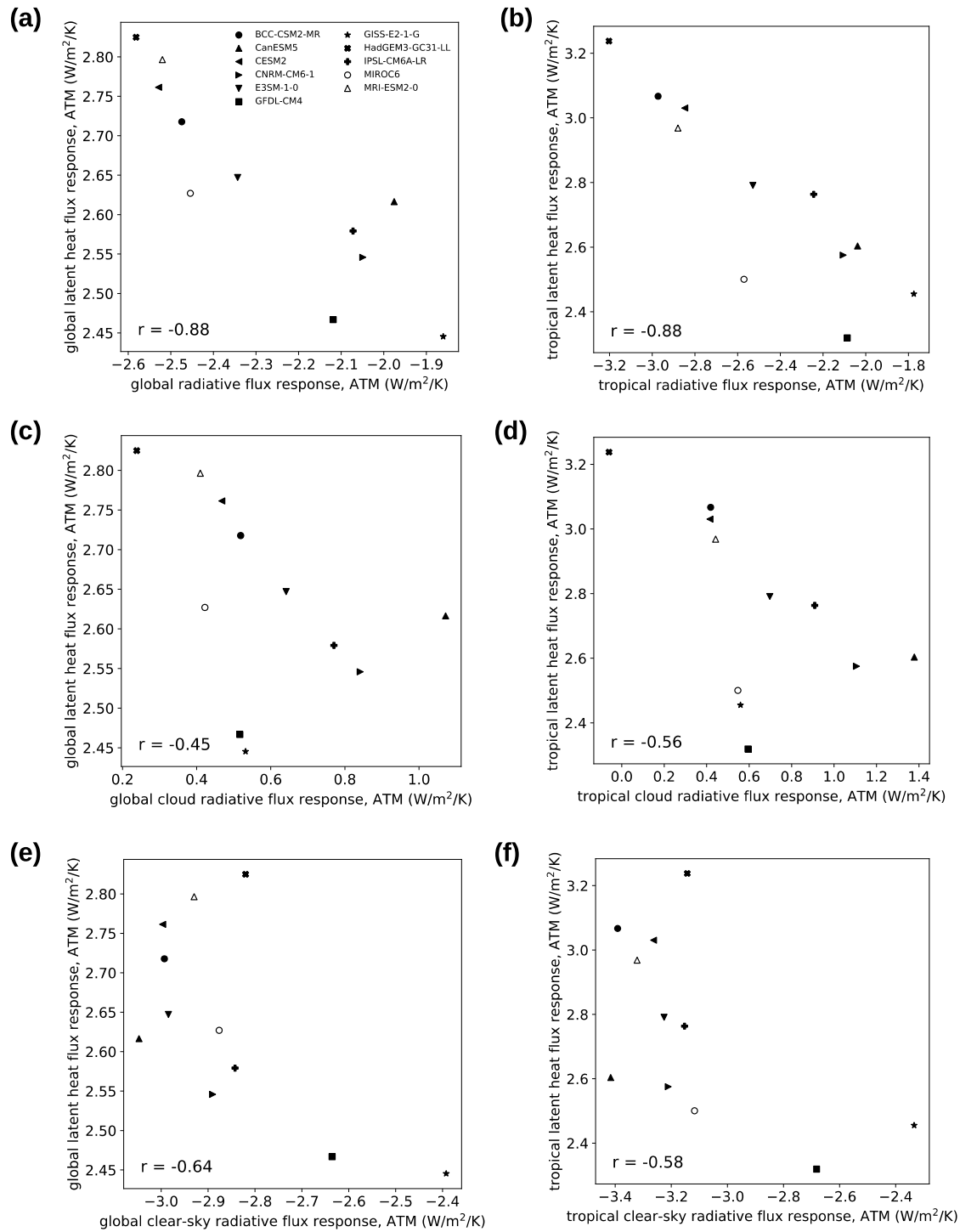


Figure S3. Correlations between radiative and precipitation (latent heat) responses to surface warming among AMIP6 models. Shown are full ATM radiative responses (a,b), ATM cloud radiative responses (c,d), and ATM clear-sky radiative responses (e,f), averaged both globally (a,c,e) and over the tropics (b,d,f). The latent heat responses shown are simply precipitation responses scaled into energetic units (LAP).

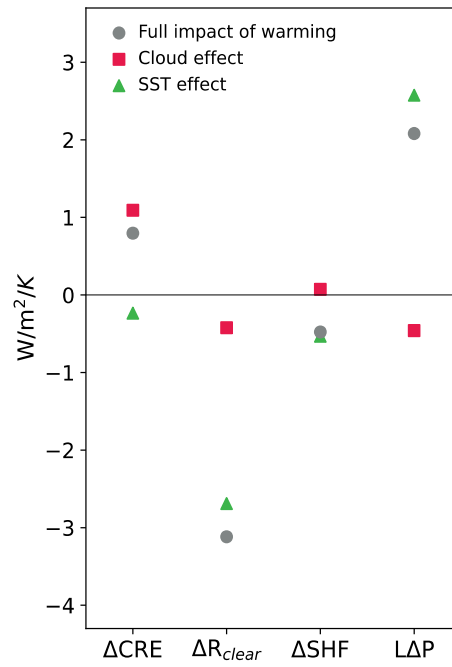


Figure S4. As in Fig. 4b but showing ICON cloud locking results averaged over the tropics (30°S to 30°N) rather than globally.

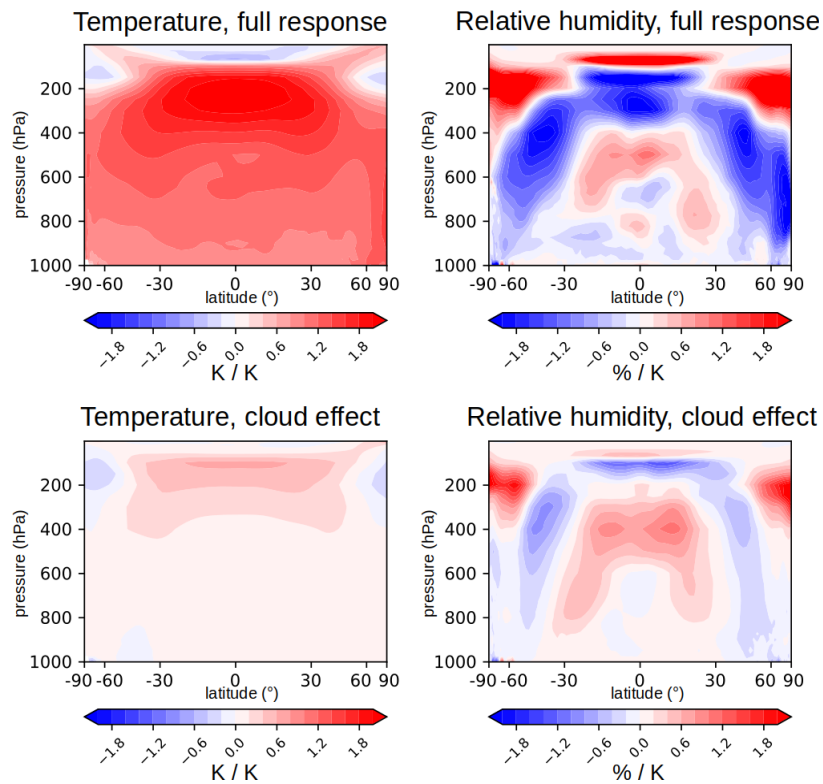


Figure S5. Atmospheric temperature and relative humidity changes in the ICON simulations, shown for both the full response (top row) and the cloud radiative effect (bottom). The cloud and SST effects shown here were calculated using Eqn. 2.

Supplementary References

Soden, B. J., Held, I. M., Colman, R., Shell, K. M., Kiehl, J. T., & Shields, C. A. (2008). Quantifying climate feedbacks using radiative kernels. *Journal of Climate*, 21(14), 3504-3520.

Yoshimori, M., Lambert, F. H., Webb, M. J., & Andrews, T. (2020). Fixed anvil temperature feedback: Positive, zero, or negative?. *Journal of Climate*, 33(7), 2719-2739.